(12) INTERNATIONAL APPLICATION PUBLISHED UNDER THE PATENT COOPERATION TREATY (PCT)

(19) World Intellectual Property Organization
International Bureau

(43) International Publication Date
02 August 2024 (02.08.2024)

WIPO | PCT

(10) International Publication Number
WO 2024/157066 A1

(51) International Patent Classification:
G01S 13/46 (2006.01) *G06N 3/02* (2006.01)
G01S 19/22 (2010.01) *G06N 3/082* (2023.01)

(21) International Application Number:
PCT/IB2023/061482

(22) International Filing Date:
14 November 2023 (14.11.2023)

(25) Filing Language: English

(26) Publication Language: English

(30) Priority Data:
300197 25 January 2023 (25.01.2023) IL

(71) Applicant: **RAFAEL ADVANCED DEFENSE SYSTEMS LTD.** [IL/IL]; P. O. B. 2250, 3102102 Haifa (IL).

(72) Inventors: **LAVI, Florin**; POB 2250, 3102102 Haifa (IL). **KALO, Ronen**; 4 Osishkint st., 2632404 Kiryat Motzkin (IL). **ZLOTNICK, Ariel**; 26 Yoni Netanyahu, 5442501 Giv'at Shmuel (IL).

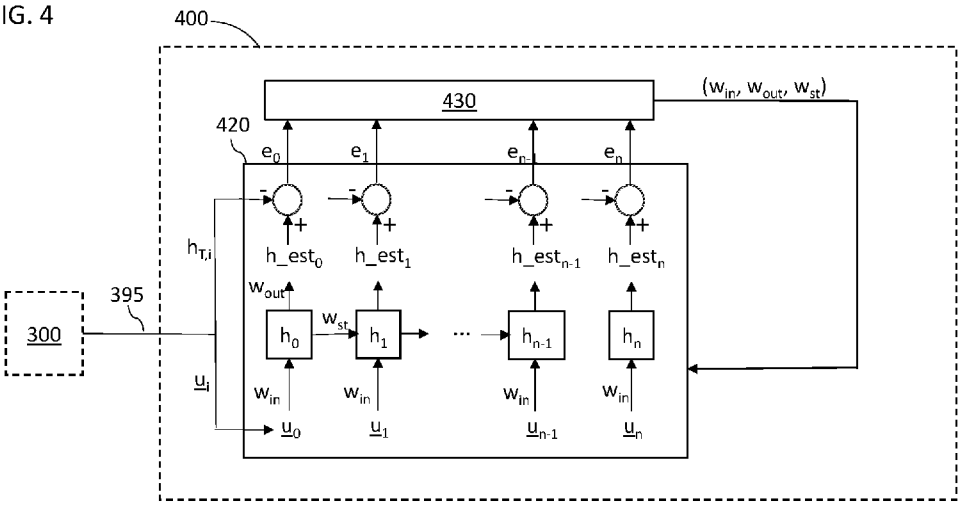
(74) Agent: **FRIEDMAN, Mark**; 7 Jabotinsky St., Moshe Aviv Tower, 54th Floor, 5252007 Ramat Gan (IL).

(81) Designated States *(unless otherwise indicated, for every kind of national protection available)*: AE, AG, AL, AM, AO, AT, AU, AZ, BA, BB, BG, BH, BN, BR, BW, BY, BZ, CA, CH, CL, CN, CO, CR, CU, CV, CZ, DE, DJ, DK, DM, DO, DZ, EC, EE, EG, ES, FI, GB, GD, GE, GH, GM, GT, HN, HR, HU, ID, IL, IN, IQ, IR, IS, IT, JM, JO, JP, KE, KG, KH, KN, KP, KR, KW, KZ, LA, LC, LK, LR, LS, LU, LY, MA, MD, MG, MK, MN, MU, MW, MX, MY, MZ, NA, NG, NI, NO, NZ, OM, PA, PE, PG, PH, PL, PT, QA, RO, RS, RU, RW, SA, SC, SD, SE, SG, SK, SL, ST, SV, SY, TH, TJ, TM, TN, TR, TT, TZ, UA, UG, US, UZ, VC, VN, WS, ZA, ZM, ZW.

(84) Designated States *(unless otherwise indicated, for every kind of regional protection available)*: ARIPO (BW, CV, GH, GM, KE, LR, LS, MW, MZ, NA, RW, SC, SD, SL, ST, SZ, TZ, UG, ZM, ZW), Eurasian (AM, AZ, BY, KG, KZ, RU, TJ, TM), European (AL, AT, BE, BG, CH, CY, CZ, DE, DK, EE, ES, FI, FR, GB, GR, HR, HU, IE, IS, IT, LT, LU, LV, MC, ME, MK, MT, NL, NO, PL, PT, RO, RS, SE, SI, SK, SM, TR), OAPI (BF, BJ, CF, CG, CI, CM, GA, GN, GQ, GW, KM, ML, MR, NE, SN, TD, TG).

(54) **Title:** NOVEL METHOD FOR TARGET HEIGHT ESTIMATION USING MULTIPATH CORRUPTED RADAR MEASUREMENTS

FIG. 4



(57) **Abstract:** A method for estimating a true height of a target from received radar signals scattered from the target and a surface in a multipath scenario, includes: deriving from a sequence of radar measurements received over a period of time successive data pairs of a measure of slant range and a multipath corrupted (MPC) target elevation; generating from the data pairs a representation of the variation of MPC target elevation with slant range over a range window having a variable length; inputting the representation to a Sequence-to-Sequence (Seq2Seq) neural network which has been trained on a dataset comprising variations of MPC target elevation with slant range for targets at different heights; and generating an estimate of the true height of the target using the trained neural network.

[Continued on next page]

WO 2024/157066 A1

Published:

— *with international search report (Art. 21(3))*

— *in black and white; the international application as filed contained color or greyscale and is available for download from PATENTSCOPE*

Novel Method for Target Height Estimation Using Multipath Corrupted Radar Measurements

FIELD OF THE INVENTION

The invention is directed to a method for mitigating the effects of multipath on radar target tracking, and specifically, to the use of a neural network to improve target height estimation.

BACKGROUND

In radar tracking of low-flying targets, the altitude of a target as measured by a monopulse radar is influenced by a phenomenon that is commonly known as "multipath". Multipath is especially severe when the main beam of the radar antenna illuminates both the target and the Earth's surface. When the range difference between the backscattered (direct ray) and one or more specularly reflected rays propagating between the target, the surface, and the radar is smaller than the radar range resolution, phase interference occurs which give rise to the large fluctuations in the apparent target elevation, known as the multi-path effect. These fluctuations depend primarily upon the instantaneous values of the radar wavelength (λ), the radar height above the surface, the true target height, and the slant range from radar to target. These fluctuations behave as a slowly changing bias which can be easily mistaken for target maneuvers.

In the prior art, multipath is generally treated as a source of angle measurement error which is to be reduced or eliminated. One approach to mitigate multipath effects is to use radar frequency diversity to average over, or "smooth", phase fluctuations at the radar. Other approaches include antenna beam null steering and the use of linear or nonlinear Kalman filters. All of these approaches have difficulty in distinguishing between slow variations in the measured target elevation which are caused by specular multipath reflections and those which are caused by actual target maneuvers in elevation.

US Patent Number 10,209,344 (hereinafter '344) to Dougherty et al., entitled "Methods and Systems for Mitigating Multipath Propagation", and dated February 19, 2019, discloses a system and method for mitigating multipath propagation which may include collecting a plurality of detections of a target, forming a plurality of models each assuming at least one parameter causing multipath propagation, determining which model best fits the detections of the target, using the best fit model to

approximate the ground conditions, and using the approximated ground conditions to remove the multipath error from the observed signals.

In the field of machine learning, a Sequence-to-Sequence (Seq2Seq) neural network is one which converts sequences from one domain to sequences in another domain. A recurrent neural network (RNN) is a type of Seq2Seq neural network in which there are connections between nodes wherein the output from some nodes affects the subsequent input to the same nodes. This enables an RNN to model the dynamics of time-varying systems and to process input data sequences of variable length.

A paper by T. Feigl et al., entitled "Recurrent Neural Networks on Drifting Time-of-Flight Measurements", published in proceedings of the IEEE 2018 International Conference on Indoor Positioning and Indoor Navigation, teaches a data-driven approach that uses training sequences to derive a near-optimal position estimator. In the presence of multipath propagation, time-of-flight (ToF) measurement errors drift due to small-scale motion. This results in changing phases of the multipath components which cause a drift in the ToF measurements. A Long Short-Term Memory RNN learns to interpret drifting errors in ToF measurements of a tracked dynamic object directly from raw ToF data.

While the above-mentioned paper by Feigl et al. describes a target location system based on RF beacon reception by a set of synchronized antennae in an indoor controlled environment having rigid walls with stationary reflective characteristics, the present invention deals with a completely different system: a moving radar in a non-stationary environment with unknown reflection and target characteristics.

SUMMARY OF THE INVENTION

This application presents a paradigm shift in the treatment of multipath for target height estimation. Rather than viewing it as a source of error or noise, the effect of multipath is leveraged based on the understanding that the large deviations around the true line-of-sight caused by multipath are deterministic in nature, with characteristic patterns when plotted vs. radar-to-target range, and contain information related to the true target altitude above the reflective surface. A dedicated neural network is constructed, which properly recognizes multipath patterns in a wide variety of radar-target scenarios, thus providing an estimate of the true target height.

For the purpose of clarity, it should be noted that, for a person skilled in the art of artificial intelligence and machine learning, any Sequence-to-Sequence (Seq2Seq) neural network could be used in the implementation.

Furthermore, the term "plot" used hereafter refers to a radar report including the current raw radar measurements of: target slant range, Doppler frequency shift, line-of-sight angles (in azimuth and elevation), and the operating RF frequency (or wavelength).

The method of the invention consists of an off-line training stage followed by a real-time stage. In the training stage, a neural network is trained and constructed to recognize multipath effects as they appear in a wide variety of off-line simulated radar-target scenarios. In the real-time stage, the neural network is used to generate an estimate of the true target height and an estimation confidence factor, based on a sliding window of multipath corrupted (MPC) raw radar data.

In contrast to other classical estimation methods, the present invention does not require any prior assumptions about the target dynamics or other stochastic parameters, such as target RCS and surface reflection coefficients.

Furthermore, in contrast with patent '344, in which multipath phenomena are handled as errors and therefore are subtracted from real-time MPC data according to a best-fit scenario [e.g. see column 6 lines 28-33 of patent '344 which recites "*Once a multipath solution has been identified over a portion of a target's path, the calculated multipath signal ... may be output to the signal correction module 18, where it is subtracted from the observed signal*"], the present invention leaves the multipath phenomena in place, and leverages the valuable information and characteristics of the multipath signal by using a pre-trained neural network for providing the target true altitude.

According to one aspect of the presently disclosed subject matter, there is provided a method for estimating a true target height from received radar signals scattered from the target and a surface in a multipath scenario. The method includes the steps of: deriving from a sequence of radar measurements received over a period of time successive data pairs of a measure of slant range and a multipath corrupted (MPC) target elevation; generating from said data pairs a representation of MPC target elevation with slant range over a range window having a variable length; inputting said representation to a Sequence-to-Sequence (Seq2Seq) neural network, said neural network being trained on a dataset comprising variations of MPC target elevation with slant range for targets at different heights; and generating an estimate of the true target height using said neural network.

According to some aspects, the neural network is a recurrent neural network (RNN).

According to some aspects, the RNN is a gated recurrent unit (GRU) neural network.

According to some aspects, the surface is a sea or land surface.

According to some aspects, the successive data pairs correspond to different radar operating wavelengths.

According to some aspects, the radar signals are those of a radar employing frequency agility techniques.

According to some aspects, the radar signals are those of a radar employing phase or amplitude monopulse techniques.

According to some aspects, the radar signals are those of a radar mounted on a moving platform.

According to some aspects, the radar measurements incorporate Doppler frequency shifts which may be used as a decision aid to differentiate between approaching, receding, or tangential target trajectories.

According to some aspects, the dataset further includes variations of MPC target elevation with slant range for targets executing maneuvers.

According to some aspects, the dataset includes variations of the MPC target elevation with slant range obtained from computer simulations and/or experimental radar recordings.

According to some aspects, the dataset further includes effects of earth curvature and/or atmospheric refraction.

According to some aspects, the neural network includes interpolation to a predetermined discrete range grid.

According to some aspects, the neural network comprises a sliding window algorithm.

According to some aspects, the sliding window algorithm includes a backwards sliding window with an adaptive history length.

According to some aspects, the method further includes generating a confidence factor corresponding to the estimate of the true height of the target.

According to another aspect of the presently disclosed subject matter, there is provided a computer-readable storage medium including computer-executable instructions that, responsive to execution by a processor, implement the method of claim 1.

According to yet another aspect of the presently disclosed subject matter, there is provided a radar system configured to implement the method of claim 1.

BRIEF DESCRIPTION OF THE DRAWINGS

The invention is herein described, by way of example only, with reference to the accompanying drawings. Like reference numerals are used to denote similar or like elements in the drawings.

FIG. 1: A definition sketch of a multipath scattering geometry.

FIG. 2A: An exemplary graph of MPC target elevation measurements vs. slant range for a non-maneuvering target.

FIG. 2B: An exemplary graph of MPC target elevation measurements vs. slant range for a target executing a maneuver.

FIG. 3: A block diagram of an exemplary algorithm for forming a training database of radar measurements corresponding to a multiplicity of multipath scenarios.

FIG. 4: A block diagram of an exemplary algorithm for training a neural network, in accordance with the invention.

FIG. 5: A block diagram of an exemplary algorithm for real-time estimation of a true target height by a neural network, in accordance with the invention.

DETAILED DESCRIPTION

FIG. 1 shows a definition sketch of a multipath scattering geometry. The X-axis is a nominal horizontal axis, representing the reflecting surface of the Earth, which can be land or sea, in a simplified "flat-earth" model that is commonly used by those skilled in the art of radar engineering.

The definitions of the geometric symbols used in FIG. 1 are given in the following table.

Table 1: Symbols used FIG. 1

R	Radar position
T	Target position
R'	Radar image position
T'	Target image position
S	Specular reflection point
h_R	Radar height
h_T	True target height
R_d	Slant range to target
x_T	Ground range to target
R_1, R_2	Specularly reflected ray path lengths
θ_d	Elevation angle of direct ray
ψ	Grazing angle of specularly reflected ray

In FIG. 1, the direct ray is represented by the segment R-T, and specularly reflected rays are denoted by the segments R-S and S-T. To observers positioned at the radar and at the target, the reflected rays appear to emanate from the target image T' and the radar image R', respectively. Note that propagation along paths R-T, R-S and S-T is bi-directional, so that there are four possible ray combinations: direct-direct, reflected-reflected, direct-reflected and reflected-direct. The dashed line 110 corresponds to the boresight of a sum channel of a monopulse radar antenna. For simplicity and clarity of presentation, the dashed line 110 is drawn as being approximately parallel to the reflecting surface represented by the x-axis, and effects due to curvature of the Earth and of electromagnetic rays refracted by the Earth's atmosphere are not shown in the simplified planar geometry of FIG. 1. When the Earth is treated as a curved surface, the term "target height" denotes the distance of the target from the surface along the local vertical direction. Methods to compensate for the effects of Earth curvature are generally well-known to those skilled in the art of radar engineering.

Radar antenna pattern 120 shows the dependence of a monopulse sum channel gain on the elevation angle relative to boresight. In monopulse radars, the radar antenna also includes a difference

channel which enables estimation of a target elevation angle by comparing the amplitude and/or phase of signals received in the sum and difference channels, using techniques that are familiar to those skilled in monopulse radar technology. The radar also measures a slant range to the target, R_d, based on a time-of-arrival of the received radar signal, using standard range-gating techniques. When the radar beam illuminates both the target and the reflective surface, the direct and reflected signals combine at the radar. If the range and Doppler frequency shift difference between the direct and reflected signals are simultaneously smaller than the radar resolution cell, interference gives rise to the MPC angular measurements errors.

Target RCS pattern 130 shows the variation of the RCS with target aspect angle. For targets consisting of multiple scattering elements, the RCS pattern 130 may be highly anisotropic. The RCS corresponding to the direct ray in the direction T-to-R is referred to as a "monostatic" RCS; and the RCS corresponding to the reflected ray in the direction T-to-S is referred to as a "bistatic" RCS.

Region 140 represents a Fresnel zone on the reflecting surface which surrounds the specular reflection point S. The complex Fresnel reflection coefficient depends, in amplitude and phase, on the frequency-dependent electromagnetic properties of the surface, including, for example, its electrical conductivity and dielectric constant. Surface roughness may give rise to diffuse reflections, which, unlike specular reflections, are amenable to mitigation by conventional averaging techniques.

FIG. 2A shows an exemplary graph of multipath corrupted (MPC) target height measurements vs. target slant range, R_d, for a non-maneuvering target, at fixed values of λ, h_R and h_T, and under variable sea state conditions. The dashed line 240 marks the ground truth which, in this example, corresponds to a target flying at a constant altitude of 150 meters above the reflecting surface. The characteristic peaks, 220a and 220b, and valleys, 230a and 230b, are caused by a phase difference, $\Delta\phi = 2\pi|\Delta R|/\lambda$, where $\Delta R=2(R_1+R_2-R_d)$ is the two-way path length difference, between the direct and reflected rays (for the reflected-reflected ray combination).

The peaks 220a and 220b, and the valleys 230a and 230b, lie on differently colored curves in FIG. 2A. The different colors correspond to different sea states. The peaks and valleys change in amplitude but their positions on the radar-to-target slant range axis are unaltered. A similar deterministic relationship holds true for other stochastic parameters of the scenario, such as the monostatic and bistatic target RCS and the surface reflection coefficients.

FIG. 2A indicates that, for fixed values of λ, h_R, and h_T, there exists a deterministic relationship between the peaks and valleys in the MPC target elevation measurement and the slant range R_d. This is a direct consequence of the physical nature of specular reflections.

FIG. 2B shows an exemplary graph of MPC target height measurements vs. target slant range for a target executing a maneuver. The sea state is constant, and the measurements are shown by the curve 250. The true target trajectory consists of level flight at a constant height of 250 meters, shown by dashed line 240a, followed by a maneuver, shown inside the dashed oval 240b, and then followed by level flight at a constant height of 850 meters, shown by line 240c. During the maneuver, the true target height increases linearly from 250 to 850 Inside oval 240b, the MPC measurements undergo rapid oscillations between peaks and valleys. The oscillations are a consequence of a rapid phase wrapping that occurs as the vertical separation increases between the target T and its image T'.

FIG. 3 shows an exemplary algorithm 300 for forming a training database of radar measurements corresponding to a multiplicity of multipath scenarios. Block 310 incorporates parameters describing a target's trajectory, such as its time dependent position, velocity and acceleration vectors, for a multiplicity of possible target maneuvers. Block 320 incorporates radar parameters, such as the wavelength, polarization, and power of the radar transmitter, the gain patterns of the sum and delta channels of the radar antenna, and the height of the radar platform above the reflecting surface of the Earth. Block 330 incorporates parameters describing the angular dependence of the monostatic and bistatic target RCS. The latter depend also on the wavelength and polarization of the radar's transmission. Block 340 incorporates parameters describing the topography of the reflecting surface, such as sea-state or terrain slope, as well as electromagnetic properties of the reflecting surface, such as Fresnel reflection coefficients which depend upon wavelength, polarization and grazing angle ψ.

Blocks 350 and 360 represent software modules which simulate the radar measurements for a given multipath scenario. The output of block 360 is validated by comparison with data collected in radar field tests, which are stored in block 370. Data-flow paths 365a and 365b represent the validation feedback loop connecting blocks 360 and 370.

Range discretization block 380 receives as input a time-series of radar measurements from block 360. The radar measurements include the radar-target slant range, R_d, the MPC target elevation and, optionally, the target Doppler frequency shift which is proportional to a time derivative of the slant range. In accordance with the dependence of the multipath bias pattern on range-height

geometry, block 380 converts and resamples the time sequence of radar measurements into discrete values corresponding to a predetermined slant range grid. The latter conversion typically requires the use of digital interpolation and re-sampling techniques, which are familiar to those skilled in the art of digital signal processing.

Range discretization block 380 outputs sequences of data triplets, which are stored in a comprehensive training database 390. Database 390 is configured to provide output to the supervised optimization process, where the output 395 includes successive values of the slant range after discretization and resampling, the MPC target height and the associated true target height (h_T).

FIG. 4 shows a block diagram of an exemplary algorithm 400 for training a neural network, in accordance with the invention. RNN 420 receives as input from database 390 a sequence $\{h_{T,i}, \underline{u}_i, i= 0, 1, \ldots n\}$, where "i" is an index of the sequence, $h_{T,i}$ is the instantaneous true target height, and $\underline{u}_i$ is a data pair whose two components are a discretized value of slant range and an MPC target height. In RNN 420, the parameters w_{in}, $w_{out,}$ and w_{st} denote weighting parameters whose values are to be determined by optimization. Each hidden state h_i is calculated as a function of the input data pair u_i to generate an estimate of true target height, h_est_i. The estimate error, $e_i = h_est_i - h_T$, is input to optimization block 430.

Optimization block 430 calculates a loss function, defined as:

$$Loss = \sum_{i=0}^{n} e_i^2 \qquad \text{(equation 1)}$$

and, using for example a first-order iterative minimization algorithm such as stochastic gradient descent, determines the optimal weights,

$$(w^*_{in}, w^*_{out}, w^*_{st}) = \underset{(w_{in}, w_{out}, w_{st})}{argmin} \; (1/k) \sum_{j=1}^{k} Loss_j \qquad \text{(equation 2)}$$

where j is an index chosen randomly from the dataset, k is the batch size for the stochastic gradient descent process, and "argmin" is a minimization over the weighting parameters w_{in}, $w_{out,}$ and w_{st}.

RNN 420 is configured to operate on sequences having variable length. An alternative embodiment of the neural network may comprise a sliding window algorithm, and the sliding window algorithm may include a backwards sliding window with an adaptive history. Furthermore, the neural network may be implemented as a gated recurrent unit (GRU) neural network.

FIG. 5 shows a block diagram of an exemplary algorithm 500 for real-time estimation of a target height by a neural network, in accordance with the invention. Radar tracking system 510 provides a time sequence of radar measurements 515a and auxiliary parameters 515b. The radar measurements 515a include target slant range and MPC target elevation angle. The auxiliary parameters 515b include instantaneous radar wavelength, λ, closing velocity (Doppler) and radar height h_R. Preprocessing block 520 performs a weighted interpolation of the radar measurements to the nearest slant range grid point and outputs a sequence of discretized data pairs to a trained RNN 530. The trained RNN provides a real-time estimate of target height, h_T_est, and an associated confidence factor, CF. The computing resources required by the trained RNN block 530 are highly efficient for real-time computation. The values of h_T_est and CF are typically fed back to a tracking algorithm which is resident in the radar tracking system 510, as indicated by paths 535a and 535b.

It will be appreciated that the above descriptions are intended only to serve as examples, and that many other embodiments are possible within the scope of the present invention as defined in the appended claims.

CLAIMS

1. A method for estimating a true height of a target from received radar signals scattered from the target and a surface in a multipath scenario, the method comprising the steps of:
   a) deriving from a sequence of radar measurements received over a period of time successive data pairs of a measure of slant range and a multipath corrupted (MPC) target elevation;
   b) generating from said successive data pairs a representation of MPC target elevation with slant range over a range window having a variable length;
   c) inputting said representation to a Sequence-to-Sequence (Seq2Seq) neural network, said neural network being trained on a dataset comprising variations of MPC target elevation with slant range for targets at different heights; and
   d) generating an estimate of the true height of a target using said neural network.
2. The method of claim 1 wherein said neural network is a recurrent neural network (RNN).
3. The method of claim 2 wherein the RNN is a gated recurrent unit (GRU) neural network.
4. The method of claim 1 wherein the surface is a sea or land surface.
5. The method of claim 1 wherein the successive data pairs correspond to different radar operating wavelengths.
6. According to some aspects, the radar signals are those of a radar employing frequency agility techniques.
7. The method of claim 1 wherein the radar signals are those of a radar employing phase or amplitude monopulse techniques.
8. The method of claim 1 wherein the radar signals are those of a radar mounted on a moving platform.
9. The method of claim 1 wherein the radar measurements incorporate Doppler frequency shifts.
10. The method of claim 1 wherein the dataset further comprises variations of the MPC target elevation with slant range for targets executing maneuvers.
11. The method of claim 1 wherein the dataset comprises variations of the MPC target elevation with slant range obtained from computer simulations and/or experimental radar recordings.
12. The method of claim 1 wherein the dataset further comprises effects of earth curvature and/or atmospheric refraction.

13. The method of claim 1 wherein the neural network includes interpolation to a predetermined discrete range grid.
14. The method of claim 1 wherein the neural network comprises a sliding window algorithm.
15. The method of claim 14 wherein the sliding window algorithm comprises a backwards sliding window with an adaptive history length.
16. The method of claim 1 further comprising generating a confidence factor associated with the estimate of the true height of the target.
17. A computer-readable storage medium comprising computer-executable instructions that, responsive to execution by a processor, implement the method of claim 1.
18. A radar system configured to implement the method of claim 1.

FIG. 1

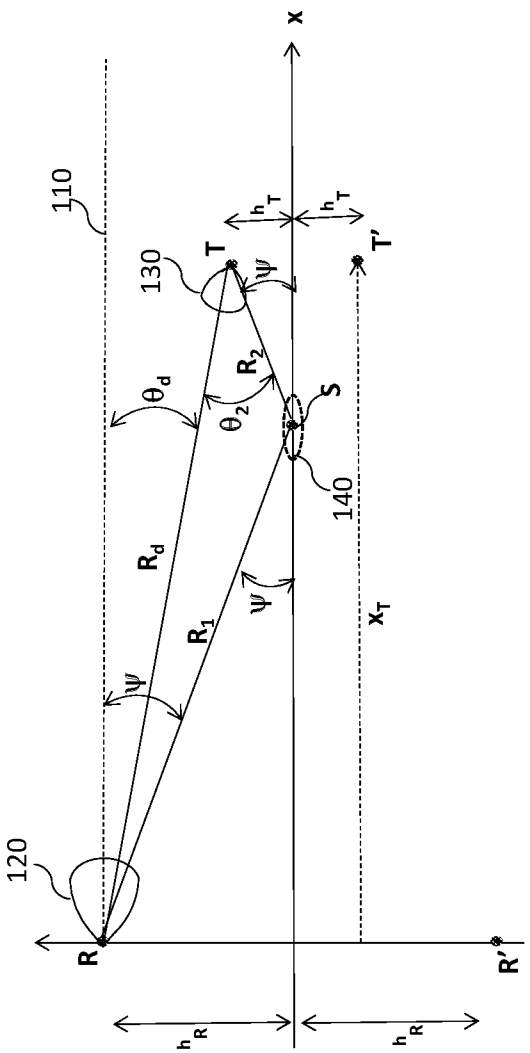


FIG. 2A

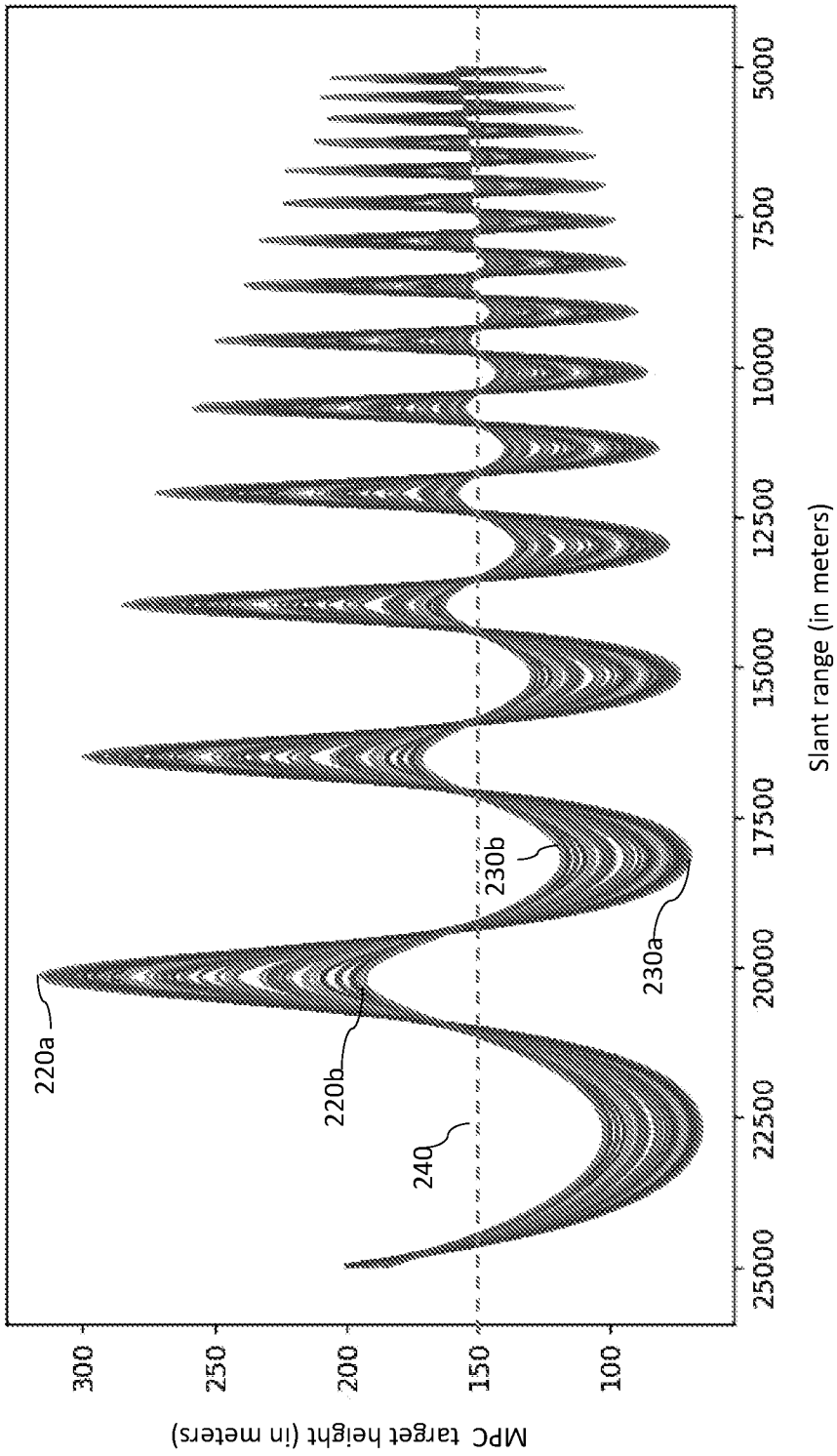

MPC target height (in meters)
300
250
200
150
100
Slant range (in meters)
25000
22500
20000
17500
15000
12500
10000
7500
5000
220a
220b
240
230b
230a

FIG. 2B

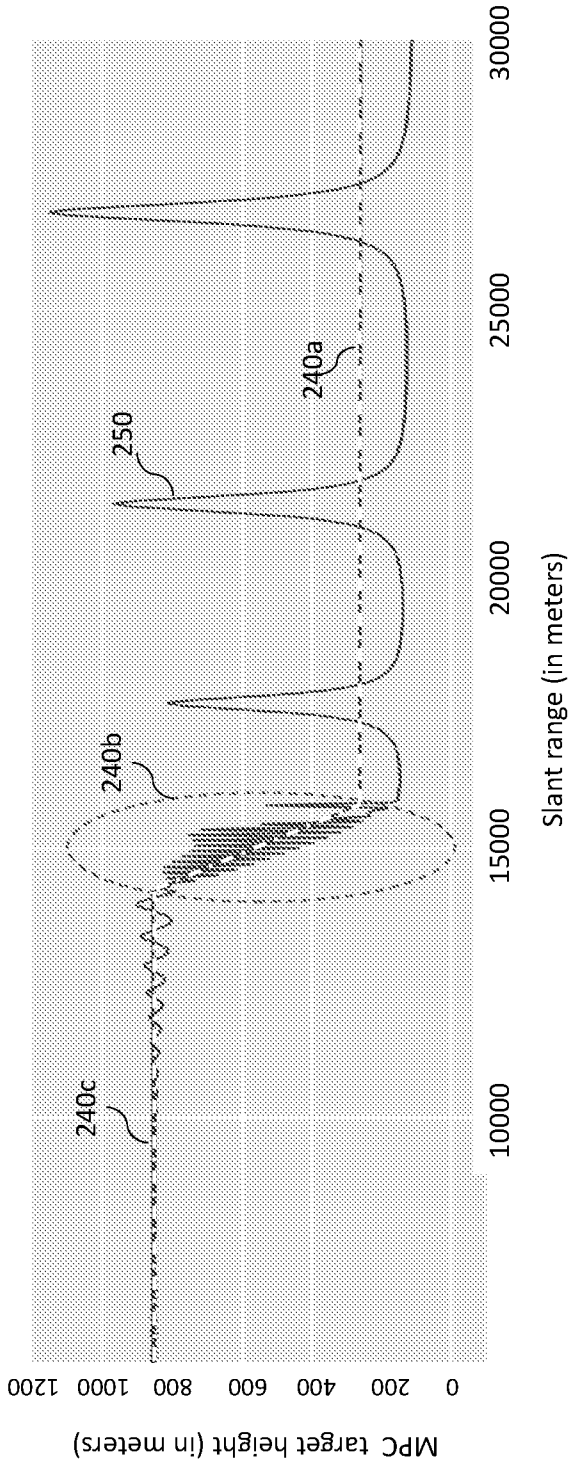

MPC target height (in meters)
0
200
400
600
800
1000
1200
Slant range (in meters)
10000
15000
20000
25000
30000
240c
240b
250
240a

FIG. 3

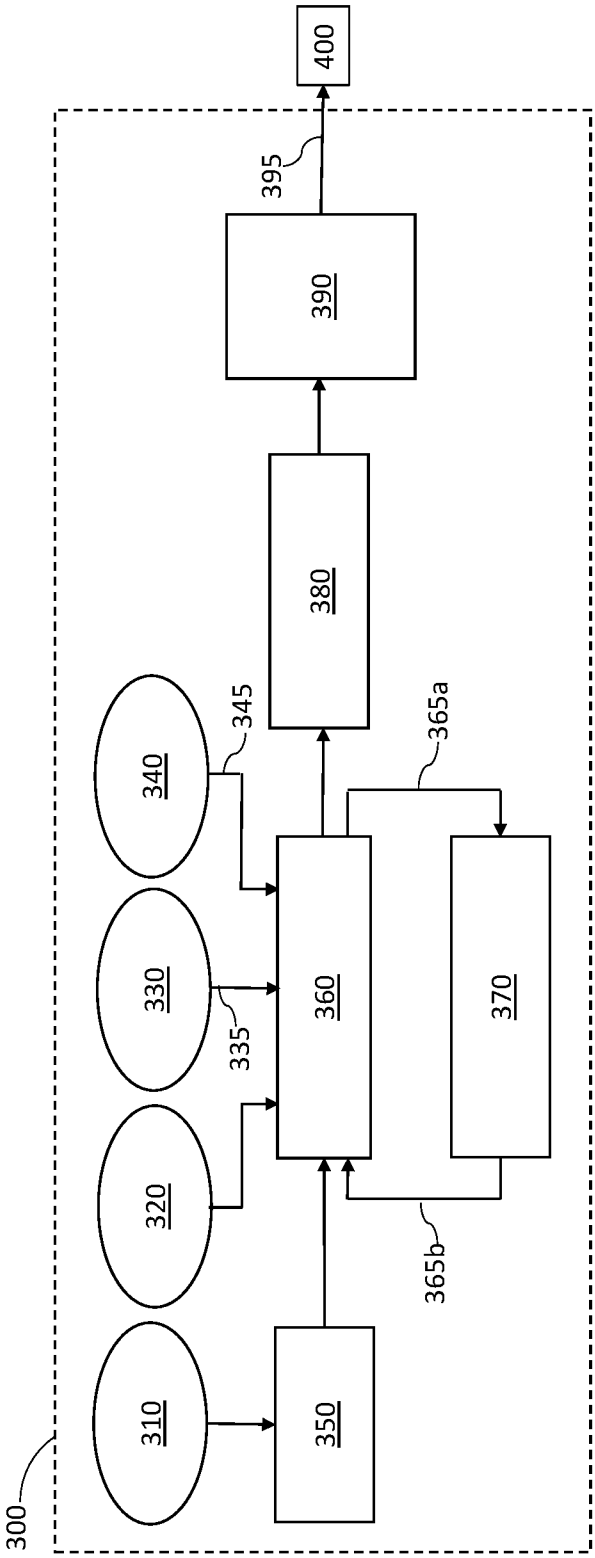

400
395
390
380
345
365a
340
330
335
360
370
320
365b
310
350
300

FIG. 4

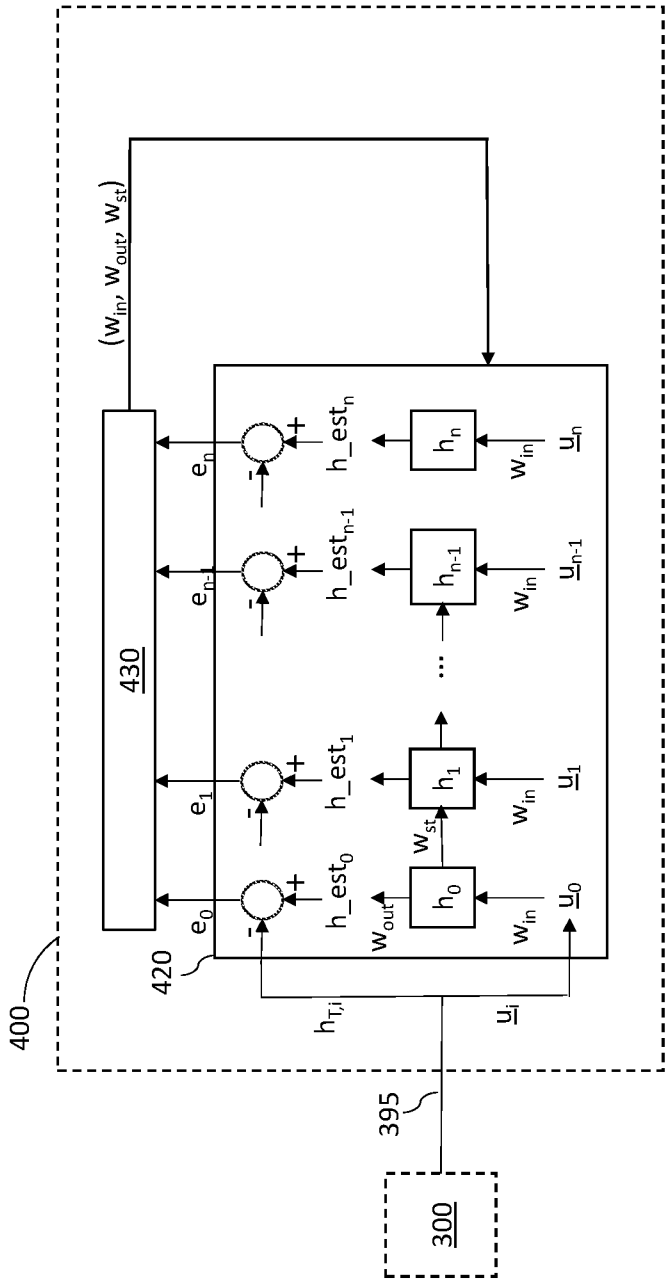
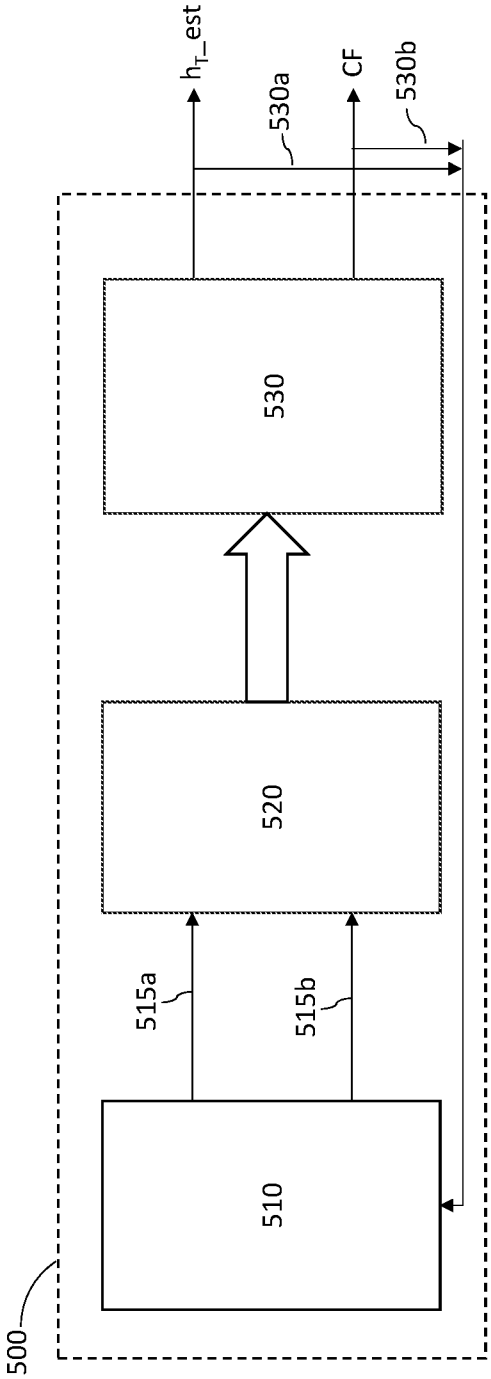

400
420
430
395
300
$(w_{in}, w_{out}, w_{st})$
$h_{T,i}$
$\underline{u}_i$
h_est_0
h_est_1
h_est_{n-1}
h_est_n
e_0
e_1
e_{n-1}
e_n
h_0
h_1
h_{n-1}
h_n
w_{out}
w_{st}
w_{in}
$\underline{u}_0$
$\underline{u}_1$
$\underline{u}_{n-1}$
$\underline{u}_n$

FIG. 5



INTERNATIONAL SEARCH REPORT

International application No.
PCT/IB2023/061482

A. CLASSIFICATION OF SUBJECT MATTER

G01S 13/46(2024.01)i; ***G01S 19/22***(2024.01)i; ***G06N 3/02***(2024.01)i; ***G06N 3/082***(2024.01)i
CPC:G01S 13/46; G01S 2013/462; G01S 19/22; G06N 3/02; G06N 3/082

According to International Patent Classification (IPC) or to both national classification and IPC

B. FIELDS SEARCHED

Minimum documentation searched (classification system followed by classification symbols)

G01S 13/46; G01S 19/22; G06N 3/02; G06N 3/082
CPC:G01S 13/46; G01S 2013/462; G01S 19/22; G06N 3/02; G06N 3/082

Documentation searched other than minimum documentation to the extent that such documents are included in the fields searched

Electronic data base consulted during the international search (name of data base and, where practicable, search terms used)

Databases consulted: Esp@cenet, Google Patents, Google Scholar, Orbit, Tdcommons Search terms used: radar, target, height, elevation, distance, location, position, trajectory, direct, indirect, multipath, measurement, data, pair, recurrent, neural, sequence,

C. DOCUMENTS CONSIDERED TO BE RELEVANT

Category*	Citation of document, with indication, where appropriate, of the relevant passages	Relevant to claim No.
A	US 2021018592 A1 (LAGHEZZA et al.) 21 January 2021 (2021-01-21) ¶ 0021, 0040	1-18
A	JP 2021532373 A ([Mitsubishi Electric Corp]) 25 November 2021 (2021-11-25) Whole document	1-18
A	US 2022269926 A1 (PAVLOV et al.) 25 August 2022 (2022-08-25) Whole document	1-18
A	CN 108828547 A ([UNIV XIDIAN]) 16 November 2018 (2018-11-16) Whole Dicument	1-18

☑ Further documents are listed in the continuation of Box C. ☑ See patent family annex.

* Special categories of cited documents:
"A" document defining the general state of the art which is not considered to be of particular relevance
"D" document cited by the applicant in the international application
"E" earlier application or patent but published on or after the international filing date
"L" document which may throw doubts on priority claim(s) or which is cited to establish the publication date of another citation or other special reason (as specified)
"O" document referring to an oral disclosure, use, exhibition or other means
"P" document published prior to the international filing date but later than the priority date claimed
"T" later document published after the international filing date or priority date and not in conflict with the application but cited to understand the principle or theory underlying the invention
"X" document of particular relevance; the claimed invention cannot be considered novel or cannot be considered to involve an inventive step when the document is taken alone
"Y" document of particular relevance; the claimed invention cannot be considered to involve an inventive step when the document is combined with one or more other such documents, such combination being obvious to a person skilled in the art
"&" document member of the same patent family

Date of the actual completion of the international search	Date of mailing of the international search report
29 January 2024	**08 February 2024**

Name and mailing address of the ISA/IL	Authorized officer
Israel Patent Office **Technology Park, Bldg.5, Malcha, Jerusalem, 9695101,** **Israel** **Israel** Telephone No. **972-73-3927223** Email: **pctoffice@justice.gov.il**	**COPPENHAGEN Uri** Telephone No.

C. DOCUMENTS CONSIDERED TO BE RELEVANT

Category*	Citation of document, with indication, where appropriate, of the relevant passages	Relevant to claim No.
A	Height Measurement of Low-Angle Target Using MIMO Radar Under Multipath Interference. IEEE TRANSACTIONS ON AEROSPACE AND ELECTRONIC SYSTEMS, 54(2). (retrieved on 01-29-2024). Retrieved from the internet: < https://www.researchgate.net/profile/Yuan_Liu218/publication/320723923_Height_Measurement_of_Low-angle_Target_Using_MIMO_Radar_Under_Multipath_Interference/links/6225e92ea39db062db8781aa/Height-Measurement-of-Low-angle-Target-Using-MIMO-Radar-Under-Multipath-Interference.pdf> LIU, Y., (2018/04/11) Whole document	1-18

INTERNATIONAL SEARCH REPORT
Information on patent family members

International application No.
PCT/IB2023/061482

Patent document cited in search report	Publication date (day/month/year)	Patent family member(s)	Publication date (day/month/year)
US 2021018592 A1	21 January 2021	US 2021018592 A1	21 January 2021
		US 11294031 B2	05 April 2022
		EP 3767333 A1	20 January 2021
		EP 3767333 B1	30 August 2023
JP 2021532373 A	25 November 2021	JP 2021532373 A	25 November 2021
		JP 7050999 B2	08 April 2022
		CN 112930484 A	08 June 2021
		EP 3665510 A1	17 June 2020
		EP 3665510 B1	28 July 2021
		US 2020132861 A1	30 April 2020
		US 11079495 B2	03 August 2021
		WO 2020090138 A1	07 May 2020
US 2022269926 A1	25 August 2022	US 2022269926 A1	25 August 2022
		CN 114972416 A	30 August 2022
		EP 4050460 A1	31 August 2022
CN 108828547 A	16 November 2018	CN 108828547 A	16 November 2018
		CN 108828547 B	29 April 2022